Hindawi
Mathematical Problems in Engineering
Volume 2023, Article ID 5533390, 14 pages
https://doi.org/10.1155/2023/5533390

Research Article

Analysis of Inherent Characteristics of Two-Speed Planetary Gear Transmission System

Wuzhong Tan,[1,2] Zhibin Zheng,[1] Xueshen Wu,[3] Enming Xiang,[1] and Yixiong Yan[4]

[1]*School of Mechanical and Electrical Engineering, Central South University, Changsha 410083, China*
[2]*AECC Hunan Aviation Powerplant Research Institute, Zhuzhou, Hunan 412002, China*
[3]*Aviation Military Representative Office of the PLA Army Equipment Department, Zhuzhou, Hunan 412002, China*
[4]*Department of Mechanical and Electrical Engineering, College of Automotive and Mechanical Engineering, Changsha University of Science and Technology, Changsha, Hunan 410114, China*

Correspondence should be addressed to Zhibin Zheng; zhengzb0526@126.com

Received 15 May 2023; Revised 20 September 2023; Accepted 21 September 2023; Published 26 October 2023

Academic Editor: Gianluca Gatti

In the helicopter transmission system, because the two-speed gear planetary transmission system without power interruption adopts the design of a double planetary gear system, the complexity of the structure leads to the time-varying meshing stiffness, tooth surface friction and the interaction between components and other nonlinear factors are uncontrollable, and causes the helicopter transmission system vibration noise, unstable operation, and other problems. To solve the above problems, the inherent characteristics of the two-speed planetary gear transmission system without power interruption were studied and analyzed to find out the influence law of its inherent characteristics. The inherent characteristics of a planetary gear drive system are mainly related to the integrated stiffness such as component mass, support stiffness, and meshing stiffness in the system. Based on the centralized mass method, the translation-torsional coupling dynamics model of the double planetary gear drive system was established. According to the displacement coordination relationship between the components of the system, the dynamics equation of the double planetary gear drive system was constructed. The mass matrix and stiffness matrix were obtained using MATLAB, and the system's natural frequency was obtained by solving the dynamics equation. The results show that the low-order natural frequency is mainly the torsional vibration mode of the center component and the torsional vibration mode of the center component. The influence of the mass of the component on the natural frequency is more complex and has a certain influence on both the high- and low-order natural frequency. The support stiffness in the system mainly affects the low-order natural frequency and the meshing stiffness in the system mainly affects the high-order natural frequency.

1. Introduction

Planetary gear transmission has the advantages of large ratio, lightweight, input and output coaxial, and power separation to improve the carrying capacity. It is widely used in transmission and reduction devices. With the development of high-performance, high-power gear transmission system, especially the two-stage planetary gear transmission system without power interruption, the structure of the planetary gear transmission system is more and more complex, and the analysis of its dynamic performance is more and more complicated. Therefore, in order to study the influence law of each factor on the dynamic performance and ensure the safety and reliability of the planetary gear system with complex structure, analyzing the intrinsic frequency of the planetary gear system is the basis of the research on the dynamics of the planetary gear system, and further provides theoretical support for the control of its vibration damping and noise and other performance.

There have been many studies on the vibration characteristics of conventional planetary gear systems. The main methods currently used to study the dynamic modeling of planetary gear systems are classified into the centralized parameter method and the finite element method. According to the finite element model established by the semianalytical finite element column type used by Ambarisha and Parker

[1], the intrinsic frequencies and vibration modes of the system in question were obtained. However, considering the complexity that follows the drive train, the dynamics modeled based on the finite element method places higher demands on high-performance hardware and software. Therefore, applications of the finite element method are rarely published [2]. Since a planetary gear system can be regarded as a point with concentrated mass, the concentrated parameter method has been applied in studies related to planetary gear systems [3]. Kahraman [4] proposed a pure torsional model for a single-stage planetary gear system and obtained the torsional intrinsic frequency equation. Kahraman [5] modeled the pure torsional dynamics of a series of composite planetary gear trains and predicted the free vibration characteristics of each configuration separately. Guo and Parker [6] modeled the rotational degrees of freedom of a general planetary gear system and investigated its intrinsic frequency and vibration pattern. Qiu et al. [7] established a unified mathematical model based on the kinematic, hydrostatic, and structural characteristics of state-space gear trains. Finally, digital identification and automatic analysis of any complex gear train are realized.

The pure torsional model only considers the rotational moments of the planetary gear system, and the model established is simple and concise. Compared with the finite element model, the pure torsional model based on the centralized mass method loses more accuracy, so it is crucial to establish a fine dynamics model with lateral-torsional coupling. And most of the studies on planetary gear systems are simple single-stage planetary gears, and there are fewer studies on multistage planetary gears, such as Abousleiman [8] proposed a model combining the lumped-parameter method and the finite element method, which is able to model the dynamical behaviors of planetary system. Gong et al. [9] developed a 23 degree of freedom translational-torsional nonlinear dynamics model based on the set-total parameter theory in order to investigate the effects of various parameters on the dynamic characteristics of a concentric face gear split-torque transmission system. Kai et al. [10] established a translational-rotational coupled dynamics model of a two-stage enclosed planetary gear set based on linear time-invariant premises to predict the intrinsic frequency and vibration modes, and realized the compounding of simple two-stage planetary gear stages through the setting of the ratio, stiffness, and other parameters, but it could not be applied to a complex planetary gear system with two speeds and no power interruptions.

Many scholars have studied the dynamic characteristics of planetary gear trains and the dynamic performance of each operating condition [4, 11–13], aiming to explore the inherent characteristics of the planetary gear system itself. Mbarek et al. [14] considered the effect of meshing stiffness and developed a 2K-H planetary gear system translational-torsional coupled nonlinear dynamics model using the centralized parameter method, and analyzed the effect of meshing stiffness on the system dynamics performance. Sun and Hu [15] developed a centralized parametric model of a multistage planetary gear system considering the effects of meshing and support stiffness and investigated the dynamic performance of the system under time-varying meshing stiffness and time-varying support stiffness. Lin and Parker [16] used two independent models, a centralized mass parameter mathematical model, and a finite element model, to investigate the nonlinear performance of planetary gears in different Wei et al. [17] developed a planetary gear transmission dynamics model using Newtonian theory, which considered key factors such as time-varying meshing stiffness, phase relations, and tooth contact characteristics, and systematically investigated gear axial overturning. Ericson and Parker [18] studied the effect of operating torque on the dynamic response of the system through experimental methods and analyzed the effect of the stiffness of planetary gear bearings on the intrinsic frequency, which was verified using finite element simulation. Ambarisha and Parker [1] and Ericson and Parker [19] discussed the tendency to combine planetary gear intrinsic frequencies into sets with similar intrinsic frequencies. Each ensemble contains the inherent frequencies of a central member rotation, translation, and planetary wheel mode. When the system parameters were changed, the intrinsic frequencies remained within the ensembles, and the clustering phenomenon was demonstrated experimentally using custom planetary gears and further investigated using numerical analysis. Among them, Xiao et al. [20] analyzed the dynamic characteristics of a two-stage planetary wheel system to establish a torsional dynamics model, studied the effects of time-varying meshing stiffness, friction, and other factors on the dynamic characteristics, and solved the vibration response by numerical methods when parametric excitation was applied. The literature [21] presented a nonlinear pure rotational dynamics model of a multistage closed planetary gear set consisting of two simple planetary stages. The model includes time-varying mesh stiffness, excitation fluctuations, and gear backlash nonlinearities. Yang et al. [22] has modeled the dynamics of a clad shell differential gear train with radial bearings by considering the time-varying meshing stiffness and the integrated transmission error factor. A translational-rotational coupled dynamics model of a two-stage enclosed planetary gear set to predict the intrinsic frequencies and vibration modes based on linear time-invariant consideration of torsion, bearing, and interstage coupling stiffness in the literature [10].

Considering that the unpowered interrupted two-speed planetary gear system directly determines the performance of a two-speed helicopter, an accurate dynamic model of the two-speed planetary gear system is needed to enhance the development of high-speed and high-performance helicopters. Therefore, on the basis of the established transverse-torsional coupled free vibration model, the study focuses on the intrinsic frequency and vibration pattern of the planetary gear system, as well as the sensitivity analysis of the factors influencing the intrinsic characteristics of the planetary gear system.

The rest of the paper is organized as follows: Section 2 introduces the dynamics model of the double planetary gear system. In this section, a translational-torsional coupled dynamics model of the planetary gear system is developed

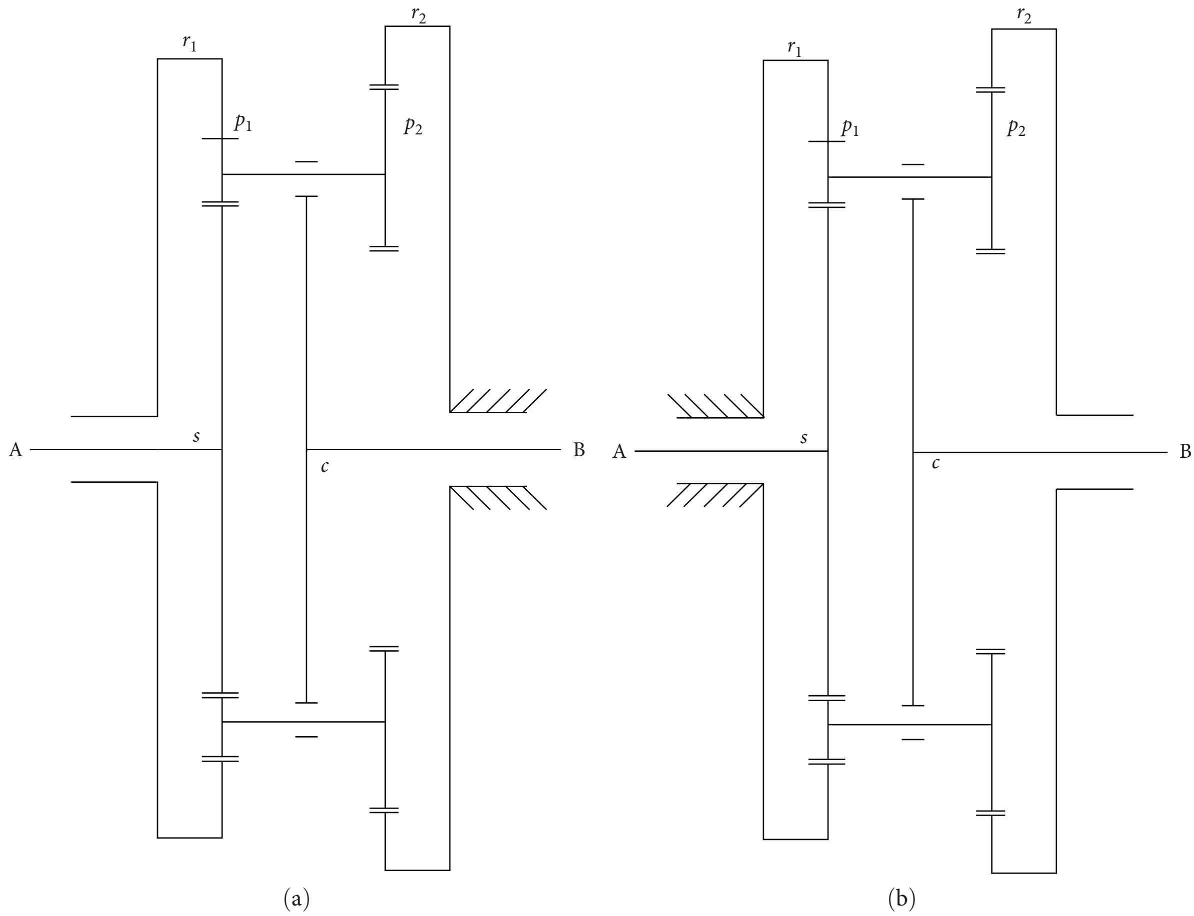

Figure 1: Schematic diagram of double planetary gear transmission mechanism. (a) High-speed gear and (b) low-speed gears.

based on the concentrated mass method, taking into account the friction of the spur gear tooth surfaces and the interaction of the components, the gear meshing stiffness. Section 3 analyzes the intrinsic characteristics for the established dynamics model and verifies the established dynamics model by finite element model. The reliability of the kinetic model is verified. The results of the sensitivity analysis of the factors affecting the intrinsic properties of the planetary gear system and a short discussion are explained in Section 4. Section 5 contains the summary and conclusion of the study.

2. Dynamics Model of Double Planetary Gear System

2.1. System Equivalent Dynamics Model. The mechanism diagram of the double planetary gear drive system is shown in Figure 1. Composed of solar wheels, double planetary gear $\boldsymbol{p_1}$–$\boldsymbol{p_2}$ (where the number of planetary wheels $\boldsymbol{n}$ can be 1, 2 … $\boldsymbol{N}$), and the first and second gear rings $\boldsymbol{r}_1$ and $\boldsymbol{r}_2$, and the planetary shelf $\boldsymbol{c}$ is constituted. Double planetary gear $\boldsymbol{p_1}$–$\boldsymbol{p_2}$ is an integral component, representing the first and second planetary gear respectively. In the system, the first stage gear ring rotates freely, the second stage gear ring is fixed, and the solar wheel and the planetary shelf are input and output components respectively, $\boldsymbol{A}$ is input and $\boldsymbol{B}$ is output.

The variable speed principle is as follows:

(1) High-speed working condition. The second row of the gear ring locks, as the second row of the gear ring has more teeth than the first row of the gear ring, at this time the first row of the gear ring rotates in the same direction as the input.

(2) Low-speed working condition. The second row of the gear ring rotates freely, and the first row of the gear ring will have the tendency to rotate in the opposite direction with the input shaft (there is one external engagement).

Figure 2 shows the parameter model of the double planetary gear transmission system based on the centralized mass method. In the parameter model, the solar wheel, double planetary gear, the first stage inner gear ring, the second stage inner gear ring, and the planetary frame are regarded as rigid bodies. The supports on and between components are simplified into springs with supporting stiffness in three directions, and the meshing between gears is simplified into springs with meshing stiffness. The damping effects at the positions of the simplified springs above are ignored because the undamped natural frequency is considered in this paper.

In Figure 2, the radial support stiffness of the solar wheel, planetary shelf, first stage and second stage inner gear, and double planetary gear in the $\boldsymbol{x}$ and $\boldsymbol{y}$ directions shown in Figure 2 are $\boldsymbol{k_{sx}}$, $\boldsymbol{k_{sy}}$, $\boldsymbol{k_{cx}}$, $\boldsymbol{k_{cy}}$, $\boldsymbol{k_{r1x}}$, $\boldsymbol{k_{r1y}}$, $\boldsymbol{k_{cnx}}$, and $\boldsymbol{k_{cny}}$.

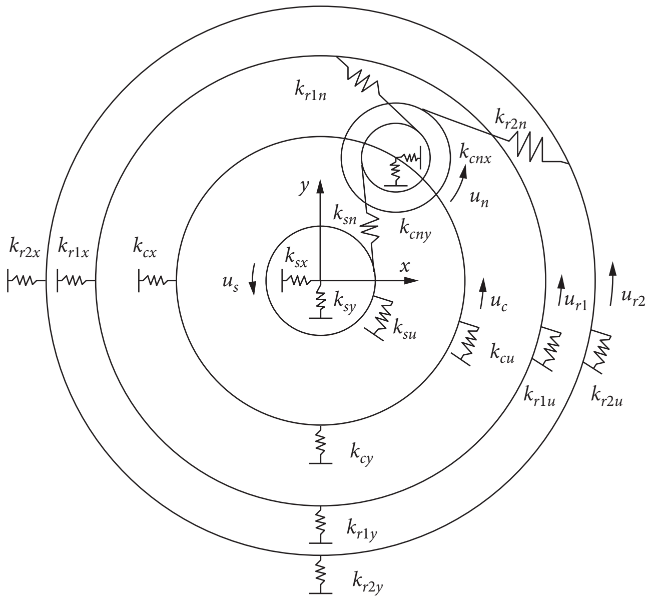

FIGURE 2: Double planetary gear system dynamics model.

Respectively, $\boldsymbol{k_{cny}}$ represents the radial support stiffness between the NTH double planetary gear and the planetary shelf, with the same size. To represent multiple meshing, $\boldsymbol{n}$ is used to represent the double planetary gear. The circumferential supporting stiffness of the solar wheel, planetary shelf, first stage, and second stage inner gear ring in the $\boldsymbol{u}$ direction is $\boldsymbol{k_{su}}$, $\boldsymbol{k_{cu}}$, $\boldsymbol{k_{r1u}}$, $\boldsymbol{k_{r2u}}$. The meshing stiffness between the solar wheel and the first stage planetary gear, the first stage planetary gear and the first stage inner gear ring, and the second stage planetary gear and the second stage inner gear ring are $\boldsymbol{k_{sn}}$, $\boldsymbol{k_{r1n}}$, $\boldsymbol{k_{r2n}}$. The circumferential displacement of the first stage planetary gear around the axis of rotation is $\boldsymbol{u_s}$, $\boldsymbol{u_c}$, $\boldsymbol{u_{r1}}$, $\boldsymbol{u_{r2}}$, and $\boldsymbol{u_n}$.

2.2. Relative Displacement between Components. Each component has displacement in the three directions shown in Figure 2, and the default direction of motion is by the three positive directions. Since the radial displacement between the two components will affect the relative displacement in the direction of the meshing line, the relative displacement equation between the components is projected along the meshing line.

The sun wheel and relative displacement between the NTH planetary gear along the meshing line direction projection:

$$\Delta sn = (x_s - x_n)\sin(\varphi_{sn}) + (y_s - y_n)\cos(\varphi_{sn}) + u_s + u_n. \tag{1}$$

The relative displacement of the NTH planetary gear and the inner gear ring $\boldsymbol{r}_1$ is projected along the meshing line:

$$\begin{aligned}\Delta nr_1 = &-(x_n - x_{r1})\sin(\varphi_{r1n}) + (y_n - y_{r1})\cos(\varphi_{r1n})\\ &+u_n - u_{r1}.\end{aligned} \tag{2}$$

The relative displacement between the inner gear ring $\boldsymbol{r}_2$ and the NTH planetary gear is projected along the meshing line:

$$\begin{aligned}\Delta r_2 n = &-(x_{r2} - x_n)\sin(\varphi_{r2n}) + (y_{r2} - y_n)\cos(\varphi_{r2n})\\ &+ u_{r2} - u_n\frac{r_{n2}}{r_{n2}}.\end{aligned} \tag{3}$$

The relative displacement of the planetary shelf and the NTH planetary gear in the $\boldsymbol{x}$, $\boldsymbol{y}$, and $\boldsymbol{u}$ directions:

$$\begin{aligned}&\Delta cnx = (x_c - x_n) - u_c\sin(\varphi_n)\\ &\Delta cny = (y_c - y_n) + u_c\cos(\varphi_n)\\ &\Delta cnu = -(x_c - x_n)\sin(\varphi_n) + (y_c - y_n)\cos(\varphi_n) + u_c\end{aligned}, \tag{4}$$

where $\boldsymbol{n}$ is the NTH double planetary gear ($\boldsymbol{n}$ can be 1, 2 … $\boldsymbol{N}$) is the first stage planetary gear when interacting with $\boldsymbol{r}_1$, or that is the second stage planetary gear when interacting with $\boldsymbol{r}_2$, $\boldsymbol{r}_{n1}$, and $\boldsymbol{r}_{n2}$ are the base circle radius of the first stage and second stage planetary gear. $\boldsymbol{x_s}$, $\boldsymbol{x_c}$, $\boldsymbol{x}_{r1}$, $\boldsymbol{x}_{r2}$, and $\boldsymbol{x_n}$ are the displacements of the solar wheel, the planetary shelf, the first stage, the second stage inner gear, and the double planetary gear along the $\boldsymbol{x}$ direction; y_s, $\boldsymbol{y_c}$, $\boldsymbol{y}_{r1}$, $\boldsymbol{y}_{r2}$, and $\boldsymbol{y_n}$ are the displacements of the above components along the $\boldsymbol{y}$ direction; $\boldsymbol{u_s}$, $\boldsymbol{u_c}$, $\boldsymbol{u}_{r1}$, $\boldsymbol{u}_{r2}$, and $\boldsymbol{u_n}$ are the displacements of the above components along the $\boldsymbol{u}$ direction.

To analyze the angle between different components and the *xy* direction, the following related derivation is carried out, $\boldsymbol{\varphi_n}$ is the angle between the center line of the NTH double planetary gear and the center wheel, and the positive direction of $\boldsymbol{x}$, $\boldsymbol{\alpha_s}$ is the external engagement angle between the first planetary gear and the center wheel $\boldsymbol{s}$, $\boldsymbol{\alpha}_{r1}$ is the internal engagement angle between the first planetary gear and the first inner gear ring $\boldsymbol{r}_1$, $\boldsymbol{\alpha}_{r2}$ is the internal engagement angle between the first planetary gear and the first inner gear ring $\boldsymbol{r}_2$, $\boldsymbol{\varphi_{sn}}$, $\boldsymbol{\varphi_{r1n}}$, $\boldsymbol{\varphi_{r2n}}$ are, respectively, the angle between the solar wheel, the first stage inner gear ring, the second stage inner gear ring and the first stage planetary gear, and the meshing line of the second stage planetary gear and the positive direction $\boldsymbol{y}$. The relationship between the above angle is as follows:

$$\begin{aligned}\varphi_n &= 2\pi(n-1)/N\\ \varphi_{sn} &= \alpha_s - \varphi_n\\ \varphi_{r1n} &= \varphi_n - \alpha_{r1}\\ \varphi_{r2n} &= \varphi_n + \alpha_{r2}\end{aligned}. \tag{5}$$

2.3. Each Component Controls the Equation. Based on the concentrated mass method, the force equilibrium equations of components in three directions are constructed. To analyze the natural frequency, the damping of the component and the input and output loads are ignored, and only the inertial force and the elastic force generated by the simplified spring are considered. The mass of the solar wheel, the planetary frame, the first stage, the second stage inner ring, and the double planetary gear are m_s, m_c, m_{r1}, m_{r2}, and m_n, respectively, and the moment of inertia are I_s, I_c, I_{r1}, I_{r2}, and I_n, respectively. The radius of rotation of each component, namely the radius of the base circle, is r_s, r_c, r_{r1}, r_{r2}, r_{n1}, and r_{n2}. r_c is the distance between the axis center of the twin planetary gear, namely the center line, and the geometric center of the planetary frame, namely the center of gravity. The differential equation of motion is obtained according to the relative displacement equation and the stress of the component.

Differential equation of solar wheel motion:

$$\begin{aligned} &m_s\,\ddot{x}_s + k_{sx}x_s + \textstyle\sum_{n=1}^{N} k_{sn}\Delta sn\sin(\varphi_{sn}) = 0\\ &m_s\,\ddot{y}_s + k_{sy}y_s + \textstyle\sum_{n=1}^{N} k_{sn}\Delta sn\cos(\varphi_{sn}) = 0\\ &\frac{I_s}{r_s^2}\,\ddot{u}_s + k_{su}u_s + \textstyle\sum_{n=1}^{N} k_{sn}\Delta sn = 0. \end{aligned} \tag{6}$$

Differential equation of planetary shelf motion:

$$\begin{aligned} &m_c\,\ddot{x}_c + k_{cx}x_c + \textstyle\sum_{n=1}^{N} k_{cn}\Delta cnx = 0\\ &m_c\,\ddot{y}_c + k_{cy}y_c + \textstyle\sum_{n=1}^{N} k_{cn}\Delta cny = 0\\ &\frac{I_c}{r_c^2}\,\ddot{u}_c + \textstyle\sum_{n=1}^{N} kcn\Delta cnu + k_{cu}u_c = 0. \end{aligned} \tag{7}$$

Differential equation of motion of the first inner gear ring:

$$\begin{aligned} &m_{r1}\,\ddot{x}_{r1} + k_{r1x}x_{r1} + \textstyle\sum_{n=1}^{N} k_{r1n}\Delta nr_1\sin(\varphi_{r1n}) = 0\\ &m_{r1}\,\ddot{y}_{r1} + k_{r1y}y_{r1} - \textstyle\sum_{n=1}^{N} k_{r1n}\Delta nr_1\cos(\varphi_{r1n}) = 0\\ &\frac{I_{r1}}{r_{r1}^2}\,\ddot{u}_{r1} + k_{r1u}u_{r1} - \textstyle\sum_{n=1}^{N} k_{r1n}\Delta nr_1 = 0. \end{aligned} \tag{8}$$

Differential equation of motion of the second inner gear ring:

$$\begin{aligned} &m_{r2}\,\ddot{x}_{r2} + k_{r2x}x_{r2} - \textstyle\sum_{n=1}^{N} k_{r2n}\Delta r_2 n\sin(\varphi_{r2n}) = 0\\ &m_{r2}\,\ddot{y}_{r2} + k_{r2y}y_{r2} + \textstyle\sum_{n=1}^{N} k_{r2n}\Delta r_2 n\cos(\varphi_{r2n}) = 0\\ &\frac{I_{r2}}{r_{r2}^2}\,\ddot{u}_{r2} + k_{r2u}u_{r2} + \textstyle\sum_{n=1}^{N} k_{r2n}\Delta r_2 n = 0. \end{aligned} \tag{9}$$

Differential equation of motion of the NTH planetary wheel:

$$\begin{aligned} &m_n\,\ddot{x}_n - k_{sn}\Delta sn\sin(\varphi_{sn}) - k_{r1n}\Delta nr_1\sin(\varphi_{r1n}) + k_{r2n}\Delta r_2 n\sin(\varphi_{r2n}) - k_{cn}\Delta cnx = 0\\ &m_n\,\ddot{y}_n - k_{sn}\Delta sn\cos(\varphi_{sn}) + k_{r_1 n}\Delta nr_1\cos\left(\varphi_{r_1 n}\right) - k_{r2n}\Delta r_2 n\cos(\varphi_{r2n}) - k_{cn}\Delta cny = 0\\ &I_n r_{n1}^{-2}\,\ddot{u}_n + k_{sn}\Delta sn\cdot r_{n1} + k_{r1n}\Delta nr_1\cdot r_{n1} - k_{r2n}\Delta r_2 n\cdot r_2 = 0. \end{aligned} \tag{10}$$

2.4. Mathematical Model of System Dynamics. To obtain the dynamic mathematical model of the double planetary gear transmission system, the kinematic differential equations above can be arranged into matrix format. In this paper, only three degrees of freedom in each component are considered, so the total degree of freedom is 3x $(4 + n)$. The free vibration equation of the system can be obtained without considering external excitation and damping.

$$M\,\ddot{q} + [K_b + K_m]q = 0, \tag{11}$$

where $\boldsymbol{M}$ is the mass matrix of the system, $\boldsymbol{K_b}$ is the support stiffness matrix of the system, K_m is the meshing stiffness matrix of the system, $\boldsymbol{K}$ is the stiffness matrix of the system, and $\boldsymbol{q}$ is the displacement vector of each component of the system: $\boldsymbol{q} = [x_s, y_s, u_s, x_c, y_c, u_c, x_{r1}, y_{r1}, u_{r1}, x_{r2}, y_{r2}, u_{r2}, x_{p1}, y_{p1}, u_{p1}, \ldots x_{pN}, y_{pN}, u_{pN}]$.

3. Inherent Characteristics of Two-Speed Planetary Gear Systems

By solving Equation (11), the mass matrix $\boldsymbol{M}$ and stiffness matrix $\boldsymbol{K}$ of the double planetary gear transmission system are obtained. Then eig function is used to calculate the eigenvalues and eigenvectors of the matrix $\boldsymbol{M}^{-1}\boldsymbol{K}$. After processing, the natural frequency value of the system and the corresponding formation coordinates of each natural frequency are obtained.

The meshing stiffness was used as the average value of the meshing time-varying stiffness of the gears. The support stiffness cannot be directly measured due to the existing conditions, so the values [8] in the literature are adopted. The parameters of the dual-planetary gear transmission system are shown in Table 1.

Based on the above analysis, the natural frequency analysis of the double planetary gear system is carried out. The first six order natural frequencies of the system and each part are shown in Table 2.

Based on the established finite element model, the intrinsic frequency results obtained from the finite element analysis are compared with the results of the analytical model. The finite element model is based on the formula from the literature [23], the network division boundary conditions according to the literature [24] in the setting of the way, the gear ring and gear teeth, and other key parts of the mesh refinement, and set the appropriate boundary conditions, in order

Table 1: Basic parameters of double planetary gear transmission system.

Parameter	Solar wheel	Annular gear r_1	Annular gear r_2	Double planetary gear		Planet carrier
Mass (kg)	4.79	12.17	12.66	2.90		3.52
Rotational inertia (kg/m)	0.0376	0.1767	0.3422	0.0039		0.0191
Base radius (mm)	102.19	144.48	173.84	21.14	50.51	131.25
Pressure angle (°)			20			–

Table 2: Planet gear trains other parts of the natural frequency (Hz).

	Natural frequency order					
	1	2	3	4	5	6
Input shaft	3,475	3,684	4,584	5,892	5,939	6,477
Planet carrier	534	608	616	1,290	1,679	2,093
Planet wheel	2,921	5,444	6,347	7,836	9,930	10,705
First stage inner gear ring	256	263	373	893	1,469	2,018
Second stage inner gear ring	257	395	471	574	616	975

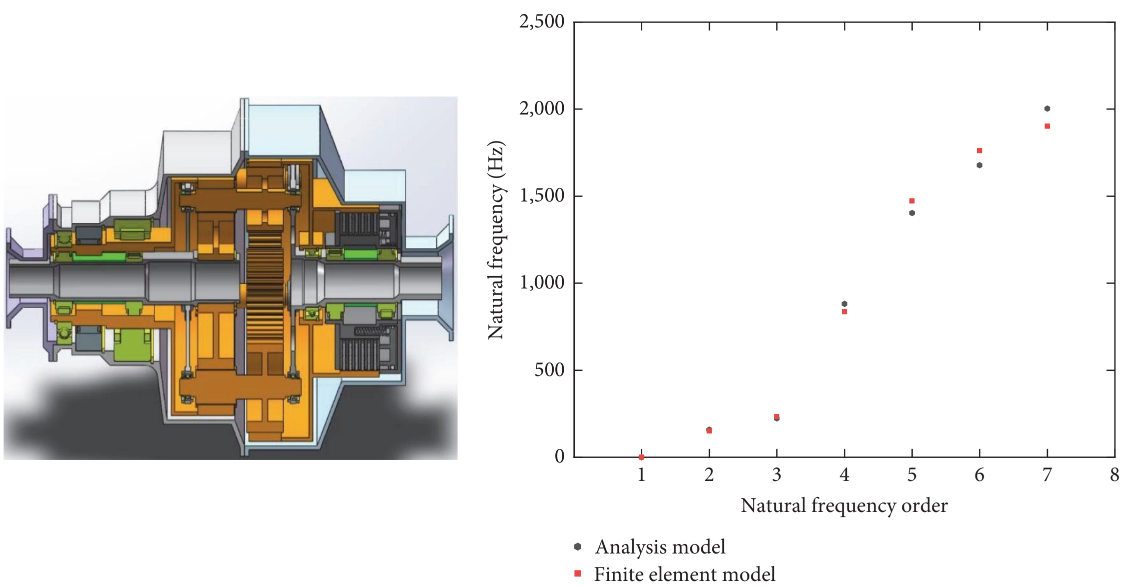

(a) (b)

Figure 3: Validation of natural frequencies. (a) Finite element model and (b) comparison of results.

to realize the high-speed gears and low-speed gears in a free-running state, the material properties and gears and other components of the setup parameters, refer to Table 1.

The specific results are shown in Figure 3, it can be seen that the inherent frequency difference between the two methods is 5%, which verifies the reliability of the analytical model. It can be seen that the inherent frequency of the two methods differs by 5%, which verifies the reliability of the analytical model. The reason for this difference may be the idealization of the boundary conditions and load conditions, the difference between the two, and the treatment of the material as a rigid body in the centralized parametric model of the gear, which is different from the finite element model.

4. Analysis of Influence Law of Dynamic Characteristics of Double Planetary Gear System

In the dynamic system without damping, the natural frequency of the system is only related to the mass and the comprehensive stiffness of each component in the system. To study the influence of the mass parameters and stiffness parameters of each component on the natural characteristics of the system. The mass and stiffness were set at 0.01 times, 0.1 times, 10 times, and 100 times equal span, and the natural frequencies $f_{0.01}$, $f_{0.1}$, f_{10}, and f_{100} before and after the change were discussed.

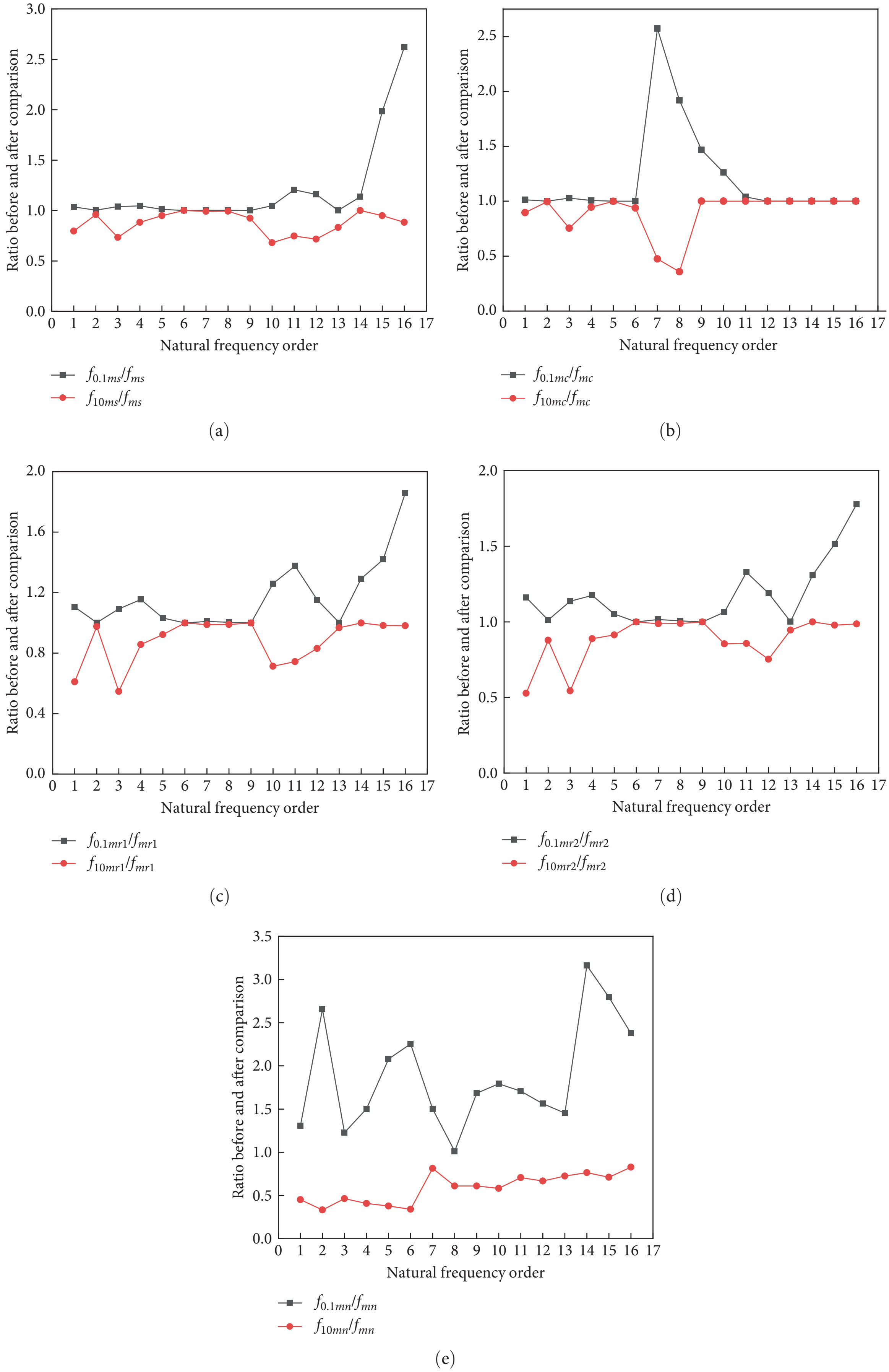

Figure 4: The influence of mass on natural characteristics of high-speed gear. (a) The solar wheel, (b) the planetary shelf, (c) the first inner ring, (d) the second inner ring, and (e) the planetary wheel.

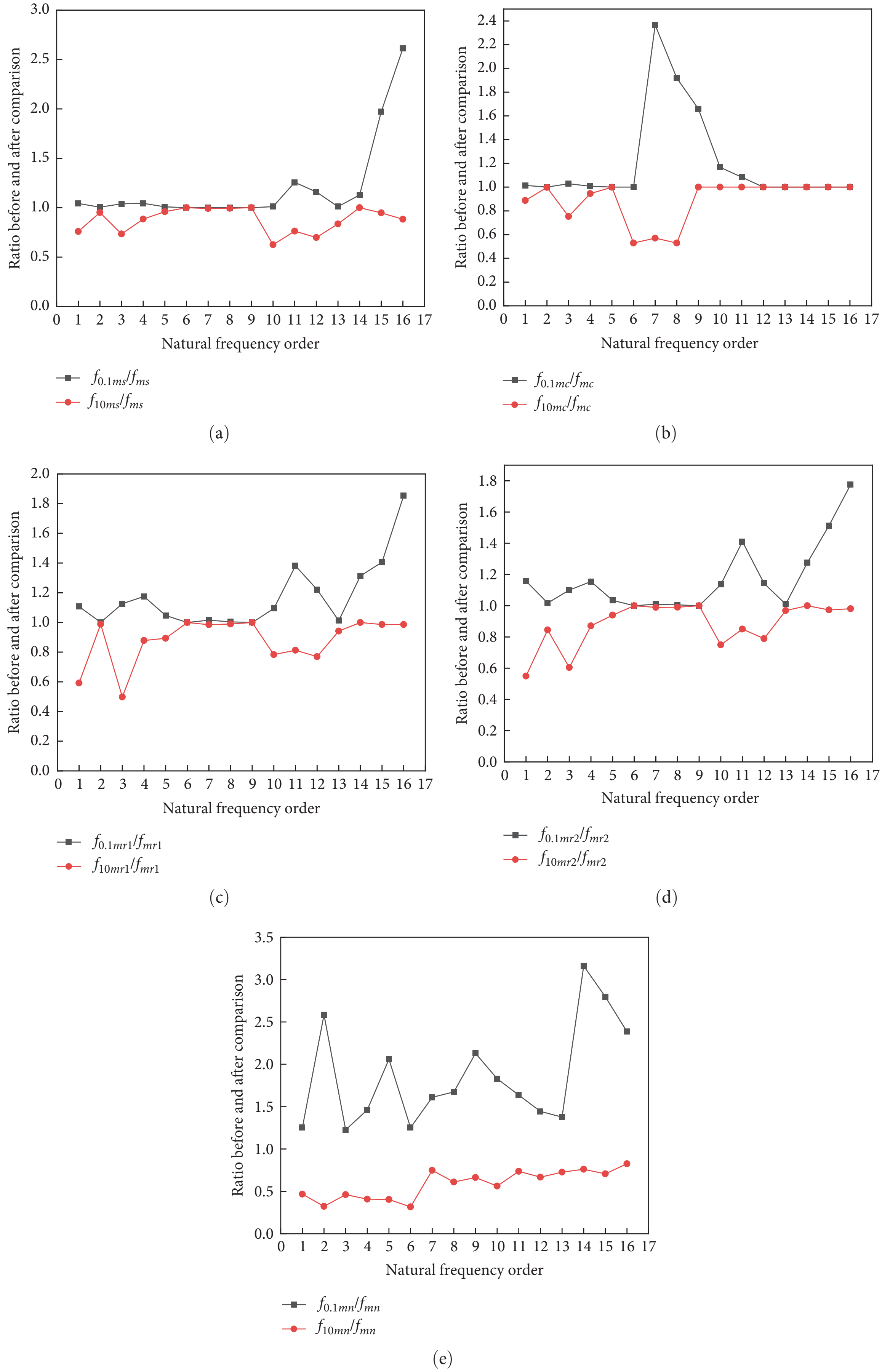

FIGURE 5: The influence of mass on natural characteristics of low-speed gear. (a) The solar wheel, (b) the planetary shelf, (c) the first inner ring, (d) the second inner ring, and (e) the planetary wheel.

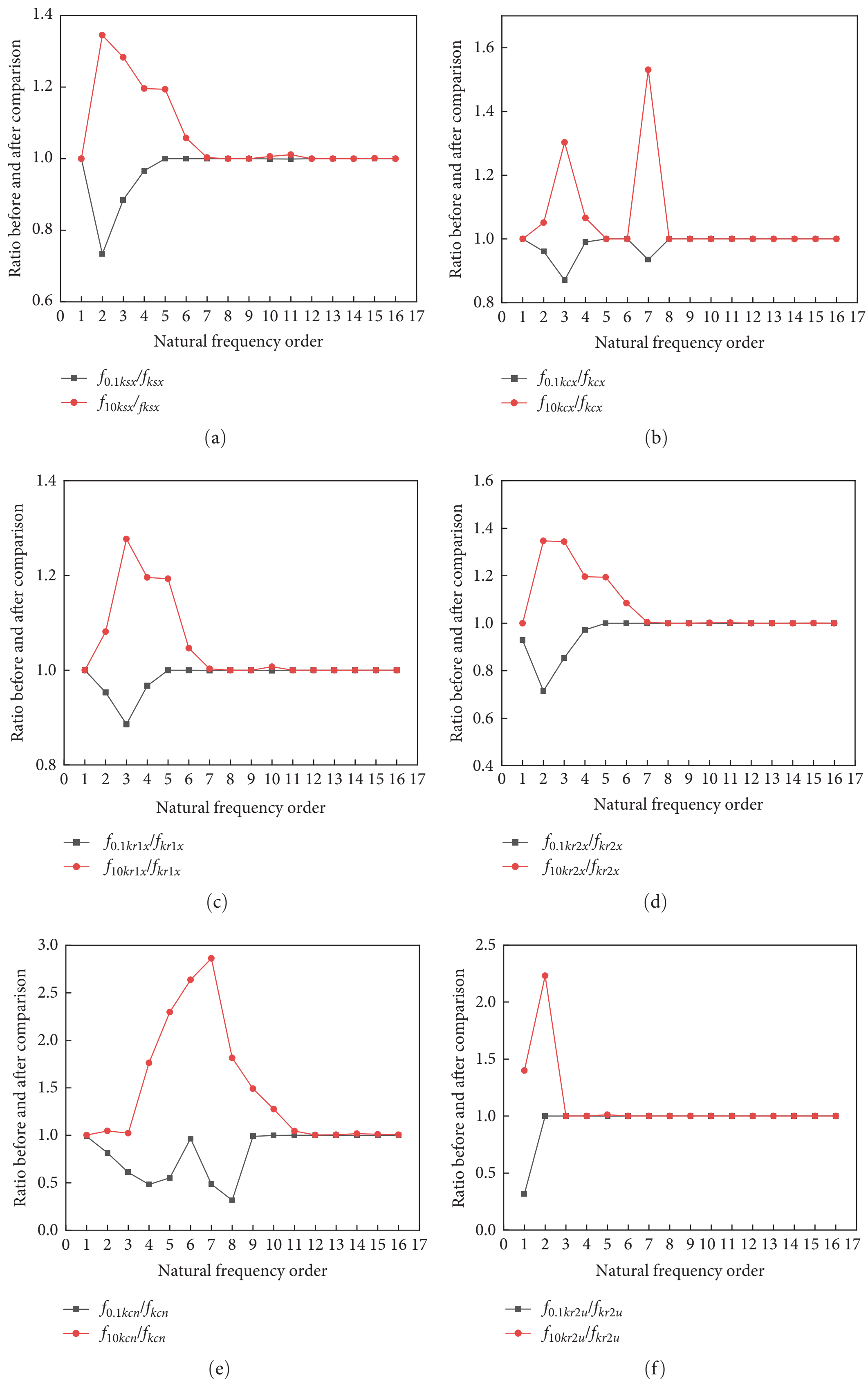

FIGURE 6: Effect of support stiffness on the inherent characteristics of high-speed gears. (a) Sun wheel, (b) planetary frame, (c) first stage gear ring, (d) second stage gear ring, (e) the planetary frame and planetary wheel, and (f) secondary internal gear ring.

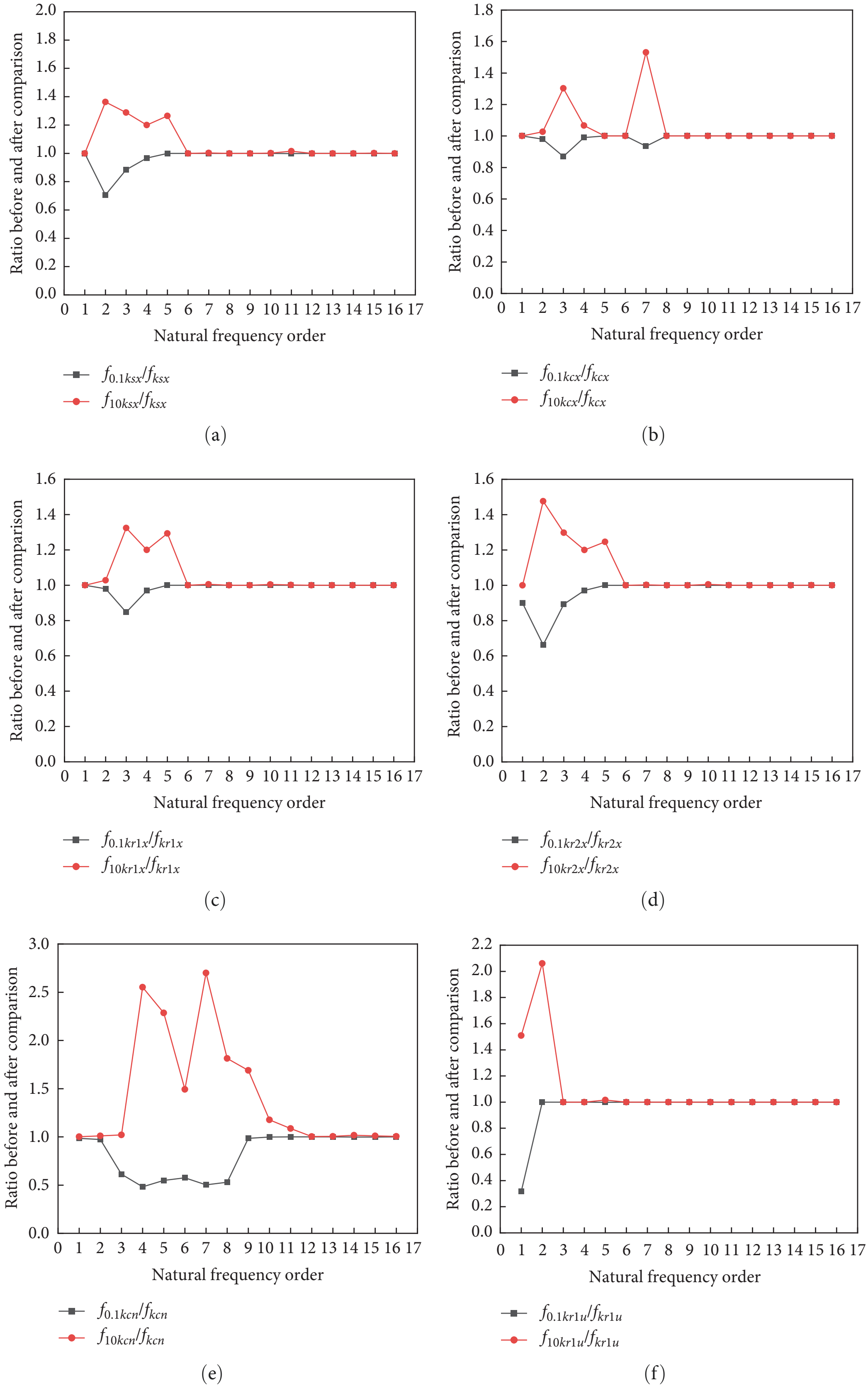

FIGURE 7: Effect of support stiffness on the inherent characteristics of low-speed gears. (a) Sun wheel, (b) planetary frame, (c) first stage gear ring, (d) second stage gear ring, (e) the planetary frame and planetary wheel, and (f) secondary internal gear ring.

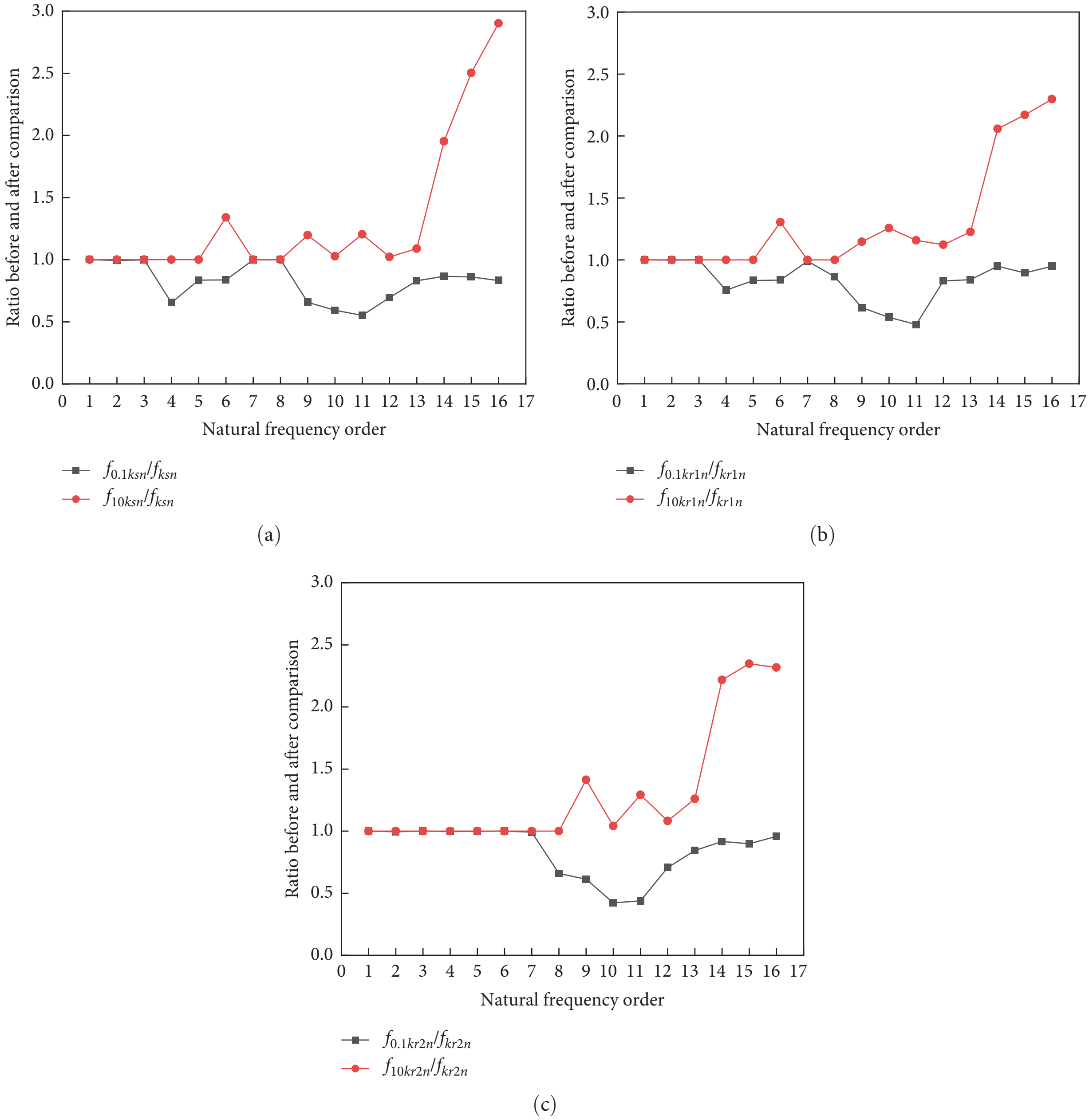

Figure 8: Effect of engagement stiffness on the inherent characteristics of high-speed gears. (a) Sun wheel and planetary gear meshing stiffness, (b) the first stage internal gear ring and planetary gear, and (c) the second stage internal gear ring and planetary gear.

4.1. Component Quality. When the mass changes, the moment of inertia also changes. The influence law of component mass on the natural frequency of the system is studied by changing the mass of the solar wheel, planetary frame, first stage, second stage inner gear ring, and planetary wheel.

4.1.1. Influence of Quality on Inherent Characteristics of High-Speed Gear. Figure 4 shows the influence law of component quality on the inherent characteristics of high-speed gear. It can be seen from the figure that the mass of the solar wheel will affect the natural frequency values of orders 1, 3–5, and 9–16, and the effect on the higher-order natural frequency values is more significant. The mass of the planetary shelf will affect the natural frequencies of orders 1, 3, and 6–10, and the effect on the natural frequencies of orders 6–10 is more significant. The quality of the first inner ring has significant effects on the natural frequencies of orders 1, 3–5, 10–12, and 14–16. The quality of the second inner gear ring will affect the natural frequency values of orders 1–5, 10–12, and 14–16, and the effect on the natural frequency values of orders 1, 3, and higher is significant. The mass of the planetary wheel has a significant effect on the natural frequency values of each order.

In summary, at high-speed gear, the mass of the solar wheel has a great influence on the high-order natural frequency, the mass of the planetary shelf has a great influence

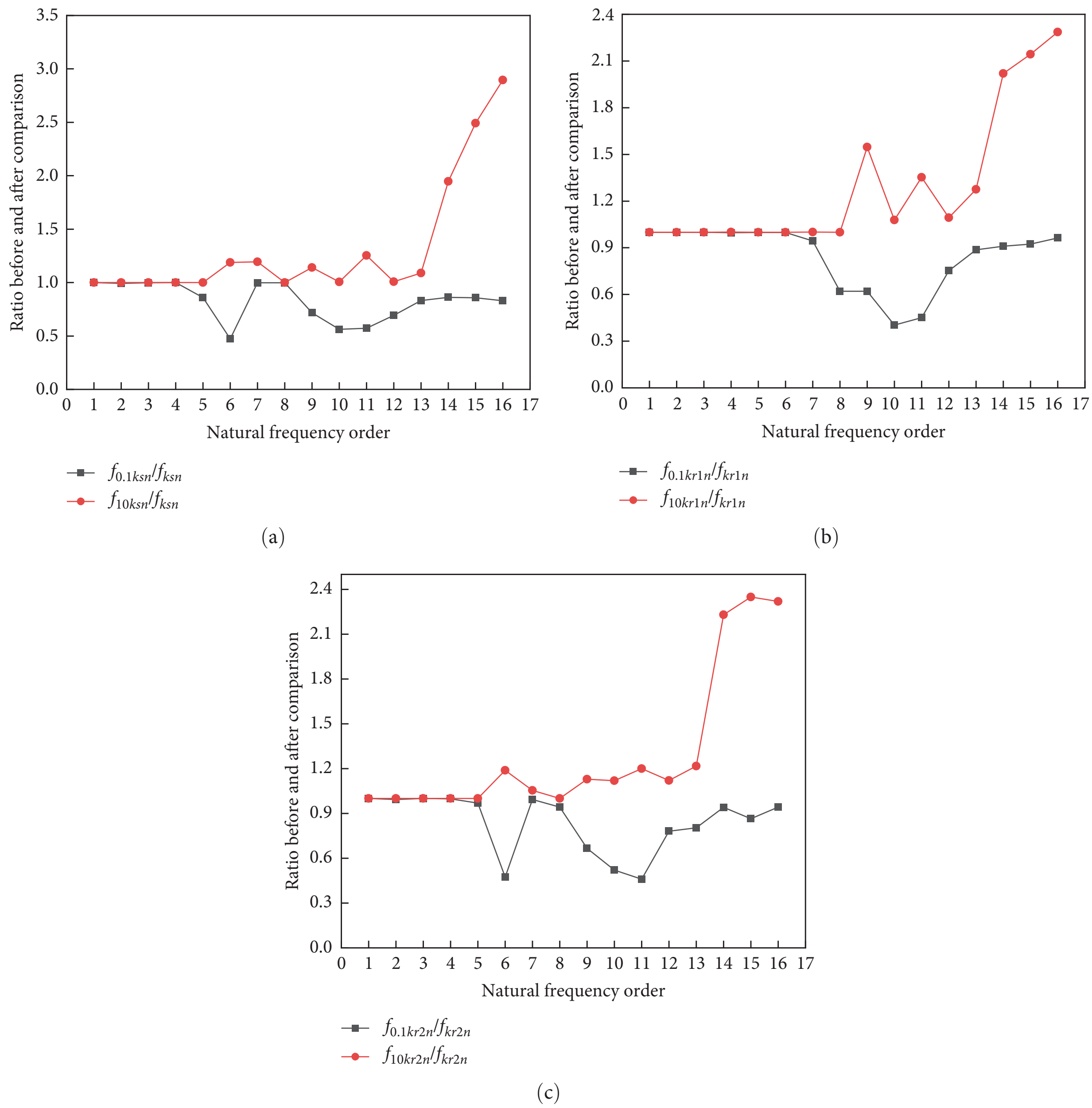

Figure 9: Effect of engagement stiffness on the inherent characteristics of low-speed gears. (a) Sun wheel and planetary gear meshing stiffness, (b) the first stage internal gear ring and planetary gear, and (c) the second stage internal gear ring and planetary gear.

on the middle-order natural frequency, the mass of the two-stage gear ring has a great influence on the high- and low-order natural frequency, and the mass of planetary wheel influences the natural frequency of each order.

4.1.2. Influence of Quality on Inherent Characteristics of Low-Speed Gear. Figure 5 shows the influence law of component quality on the inherent characteristics of low-speed gear. It can be seen from the figure that the mass of the solar wheel will affect the natural frequency values of orders 1, 3–4, and 10–16, and the effect on the higher-order natural frequency values is more significant. The mass of the planetary shelf will affect the natural frequencies of orders 1, 3, and 6–10, and the effect on the natural frequencies of orders 6–10 is more significant. The quality of the first inner ring has significant effects on the natural frequencies of orders 1, 3–5, 10–12, and 14–16. The quality of the second inner gear ring will affect the natural frequency values of orders 1–5, 10–12, and 14–16, and the effect on the natural frequency values of orders 1, 3, and higher is significant. The mass of the planetary wheel has a significant effect on the natural frequency values of each order.

In summary, at low speed, the mass of the solar wheel has a great influence on the high-order natural frequency, the mass of the planetary shelf has a great influence on the middle-order natural frequency, the mass of the two-stage gear ring has a great influence on the high- and low-order natural frequency, and the mass of the planetary wheel influences the natural frequency of each order.

4.2. Support Stiffness

4.2.1. Influence of Support Stiffness on Natural Characteristics of High-Speed Gear. It can be seen from Figure 6 that the radial support stiffness of the solar wheel affects the natural frequency values of orders 2–6. The radial stiffness of the planetary shelf will affect the natural frequencies of orders 2–4 and 7. The radial support stiffness of the first inner gear ring will affect the natural frequencies of orders 2–6. The radial support stiffness of the second inner gear ring will affect the natural frequencies of orders 1–6. The stiffness of the radial support between the planetary shelf and the twin planetary gear will affect the natural frequencies of orders 2–10. The circumferential supporting stiffness of the second inner gear ring will affect the natural frequencies of orders 1–2. It can be seen that, at high-speed gear, the radial supporting stiffness of the planetary gear system has a great influence on the first eight natural frequencies of the system, and the circumferential supporting stiffness of the planetary gear system has a great influence on the first two natural frequencies of the system.

4.2.2. Influence of Support Stiffness on Natural Characteristics of Low-Speed Gear. As can be seen from Figure 7, the radial support stiffness of the solar wheel affects the natural frequency values of orders 2–5. The radial stiffness of the planetary shelf will affect the natural frequencies of orders 2–4 and 7. The radial support stiffness of the first stage inner gear ring will affect 2–5 natural frequencies. The radial support stiffness of the second inner gear ring will affect the natural frequencies of order 1–5. The stiffness of the radial support between the planetary shelf and the double planetary gear will affect the natural frequencies of order 3–11. The circumferential supporting stiffness of the second inner gear ring will affect the natural frequencies of order 1–2.

It can be seen that, at low speeds, radial support stiffness basically has a great influence on the first eight orders of natural frequency, and circumferential support stiffness only has a great influence on the first two orders of natural frequency.

4.3. Mesh Stiffness

4.3.1. Influence of Mesh Stiffness on Natural Characteristics of High-Speed Gear. As can be seen from Figure 8, the meshing stiffness between solar gear and planetary gear will affect the natural frequencies of orders 4–6 and orders 9–16. The meshing stiffness between the first gear ring and the planetary gear will affect the natural frequencies of order 4–6 and 8–16. The meshing stiffness between the second inner ring and the planetary gear will affect the natural frequencies of order 8–16. The results show that the meshing stiffness has no effect on the first three natural frequencies at high speed, and the effect of meshing stiffness on the higher natural frequencies is more significant than that on the lower natural frequencies.

4.3.2. Influence of Mesh Stiffness on Natural Characteristics of Low-Speed Gear. As can be seen from Figure 9, the meshing stiffness between solar gear and planetary gear will affect the natural frequencies of orders 5–7 and 9–16. The meshing stiffness between the first gear ring and the planetary gear will affect the natural frequencies of order 7–16. The meshing stiffness between the second gear ring and the planetary gear will affect the natural frequencies of order 5–16. The results show that the meshing stiffness has no effect on the first four natural frequencies at low speed, and the effect of meshing stiffness on the higher natural frequencies is more significant than that on the lower natural frequencies.

5. Conclusion

Through the established dynamic model of the double-gear planetary transmission system, the influence law of each component and the system's intrinsic frequency is derived. The research results are expected to provide theoretical guidance for the structural design and working condition selection of the double-gear planetary transmission system. It is of wide significance for the optimization of helicopter transmission system performance, and further plays a significant role in vibration damping and noise control in the transmission system.

(1) The parts quality of the system has a certain influence on the high and low order of natural frequency, among which the mass of the solar wheel, the first stage, and the second stage inner gear ring has a greater influence on the higher-order frequency, the mass of the planetary frame has a greater influence on the middle order frequency, and the planetary gear has a greater influence on all the frequencies.

(2) The support stiffness of the system has a greater influence on the natural frequency of the low-order system.

(3) The meshing stiffness of the system has a greater influence on the high-order natural frequency of the system.

(4) Considering that the system generally pays more attention to low-order natural frequencies, when resonance occurs in the current system, the system dynamics characteristics are optimized mainly by changing the mass of corresponding components and the supporting stiffness of the system, especially the supporting stiffness of the second stage inner gear ring.

Data Availability

All data, models, and codes generated or used during the study are included within the article.

Conflicts of Interest

The authors declare that there are no conflicts of interest regarding the publication of this paper.

Acknowledgments

This study was supported by the National Natural Science Foundation of China (grant no. 52075552) and the Open Research Fund of State Key Laboratory of High-Performance Complex Manufacturing, Central South University (Kfkt2022-14). The authors acknowledge facility resources and support provided by the State Key Laboratory of High-Performance Complex Manufacturing, Central South University.

References

[1] V. K. Ambarisha and R. G. Parker, "Nonlinear dynamics of planetary gears using analytical and finite element models," *Journal of Sound and Vibration*, vol. 302, no. 3, pp. 577–595, 2007.

[2] W. Xu Y. Song, C. Zhang, and S. Wang, "Modified torsional model development and natural characteristics analysis of 2K-H epicyclic gearing," *Journal of Mechanical Engineering*, vol. 42, no. 5, pp. 16–21, 2006.

[3] S. Wu and H. Ren, "Research advances for dynamics of planetary gear trains," *Engineering Journal of Wuhan University*, vol. 43, no. 3, pp. 398–403, 2010.

[4] A. Kahraman, "Natural modes of planetary gear trains," *Journal of Sound and Vibration*, vol. 173, no. 1, pp. 125–130, 1994.

[5] A. Kahraman, "Free torsional vibration characteristics of compound planetary gear sets," *Mechanism and Machine Theory*, vol. 36, no. 8, pp. 953–971, 2001.

[6] Y. Guo and R. G. Parker, "Purely rotational model and vibration modes of compound planetary gears," *Mechanism and Machine Theory*, vol. 45, no. 3, pp. 365–377, 2010.

[7] J. Qiu, D. Wang, and H. Dong, "Unified mathematical model of gear train analysis based on state space method," *Mathematical Problems in Engineering*, vol. 2022, Article ID 6136899, 9 pages, 2022.

[8] W. Yang and X. Tang, "Research on the vibro-acoustic propagation characteristics of a large mining two-stage planetary gear reducer," *International Journal of Nonlinear Sciences and Numerical Simulation*, vol. 22, no. 2, pp. 197–215, 2021.

[9] F. Gong, R. Zhu, P. Li, and J. Li, "Analysis of nonlinear vibration characteristics of the concentric face-gear split-torque transmission system," *Mathematical Problems in Engineering*, vol. 2022, Article ID 1977367, 18 pages, 2022.

[10] W. Kai, W. Yong, Z. Lina, H. Qilin, and S. Ruoyu, "Dynamic modeling and vibration characteristics of a two-stage closed-form planetary gear train," *Mechanism and Machine Theory*, vol. 97, pp. 12–28, 2016.

[11] W. Kim, J. Y. Lee, and J. Chung, "Dynamic analysis for a planetary gear with time-varying pressure angles and contact ratios," *Journal of Sound and Vibration*, vol. 331, no. 4, pp. 883–901, 2012.

[12] Z. Jianxing, S. Wenlei, C. Li, and W. Guangrui, "Vibro-impact characteristics of planetary gear transmission," *Journal of Xi'an Jiaotong University*, vol. 50, no. 3, pp. 16–21, 2016.

[13] A. Hu, S. Liu, L. Xiang, and Y. Zhang, "Dynamic modeling and analysis of multistage planetary gear system considering tooth crack fault," *Engineering Failure Analysis*, vol. 137, Article ID 106408, 2022.

[14] A. Mbarek, A. F. Del Rincon, A. Hammami et al., "Comparison of experimental and operational modal analysis on a back to back planetary gear," *Mechanism and Machine Theory*, vol. 124, pp. 226–247, 2018.

[15] T. Sun and H. Y. Hu, "Nonlinear dynamics of a planetary gear system with multiple clearances," *Mechanism and Machine Theory*, vol. 38, no. 12, pp. 1371–1390, 2003.

[16] J. Lin and R. G. Parker, "Planetary gear parametric instability caused by mesh stiffness vibration," *Journal of Sound and Vibration*, vol. 249, no. 1, pp. 129–145, 2002.

[17] J. Wei, A. Zhang, D. Qin et al., "A coupling dynamics analysis method for a multistage planetary gear system," *Mechanism and Machine Theory*, vol. 110, pp. 27–49, 2017.

[18] T. M. Ericson and R. G. Parker, "Experimental measurement of the effects of torque on the dynamic behavior and system parameters of planetary gears," *Mechanism and Machine Theory*, vol. 74, pp. 370–389, 2014.

[19] T. M. Ericson and R. G. Parker, "Natural frequency clusters in planetary gear vibration," *Journal of Vibration and Acoustics*, vol. 135, no. 6, Article ID 061002, 2013.

[20] Z. Xiao, F. Chen, and K. Zhang, "Analysis of dynamic characteristics of the multistage planetary gear transmission system with friction force," *Shock and Vibration*, vol. 2021, Article ID 8812640, 10 pages, 2021.

[21] Q. Huang, Y. Wang, Z. Huo, and Y. Xie, "Nonlinear dynamic analysis and optimization of closed-form planetary gear system," *Mathematical Problems in Engineering*, vol. 2013, Article ID 149046, 12 pages, 2013.

[22] J. Yang, Y. Yue, R. Zhu, W. Chen, and M. Li, "Dynamic characteristics of encased differential gear train with journal bearing," *Mathematical Problems in Engineering*, vol. 2020, Article ID 2436191, 15 pages, 2020.

[23] J. Lin and R. G. Parker, "Structured vibration characteristics of planetary gears with unequally spaced planets," *Journal of Sound and Vibration*, vol. 233, no. 5, pp. 921–928, 2000.

[24] P.-Y. Qian, Y.-L. Zhang, G. Cheng, S.-R. Ge, and C.-F. Zhou, "Model analysis and verification of 2K-H planetary gear system," *Journal of Vibration and Control*, vol. 21, no. 10, pp. 1946–1957, 2015.